Proceedings of ALGORITMY 2020
pp. 191–200

NUMERICAL SOLUTION OF THE 1D VISCOUS BURGERS' AND TRAFFIC FLOW EQUATIONS BY THE INFLOW-IMPLICIT/OUTFLOW-EXPLICIT FINITE VOLUME METHOD *

GERGŐ IBOLYA AND KAROL MIKULA†

Abstract. In this article we solve numerically the one-dimensional viscous Burgers' equation by the inflow-implicit/outflow-explicit method. The method is based on finite volume space discretization and a semi-implicit discretization in time. Inflows to the cells are treated implicitly and outflows explicitly. Comparisons of numerical solutions with the exact ones are presented. As a physical interpretation of the Burgers' equation we chose a simple continuum traffic flow model.

Key words. viscous Burgers' equation, traffic flow, nonlinear conservation laws, finite volume method, semi-implicit scheme

AMS subject classifications. 35K20, 35L04, 35L60, 76M12, 76R50, 65M08.

1. Introduction.

Let us consider the one dimensional viscous Burgers' equation

$$u_t + uu_x = \sigma u_{xx} \tag{1.1}$$

where $\sigma \geq 0$ is the diffusion coefficient (or kinematic viscosity in a fluid dynamics context). It captures some key features of the equations of fluid dynamics: nonlinear advection, arising from the advective acceleration term in the conservation of linear momentum equation, and viscosity [1]. Another interesting interpretation of the equation (1.1) arises from simple traffic flow models, as discussed later. The equation can be solved analytically by transforming it to the linear heat equation, known as the Cole-Hopf transformation [2, 9]. This fact allows us to compare numerical solutions with the exact solution. By studying the behaviour of its numerical solutions, we can predict the performance of a particular numerical scheme on the more complicated equations of fluid dynamics.

In this paper we apply the inflow-implicit/outflow-explicit (IIOE) scheme to the nonlinear advection term of equation (1.1). The method is based on finite volume space discretization and a semi-implicit discretization in time. Inflows to the cells are treated implicitly and outflows are treated explicitly. We could explain this idea intuitively that we know what is flowing out from a cell at a given time but leave the method to resolve a system of equations determined by the inflows to obtain the solution values at the new time step. The IIOE scheme is formally second order accurate in space and time for 1D advection problems with variable velocity [5]. Combining with the Crank-Nicolson scheme for the diffusion term, we get a new numerical scheme for the nonlinear advection-diffusion problem (1.1) considered in this article.

1.1. Traffic flow.

In order to show how the viscous Burgers' equation (1.1) appears in modelling the flow of cars on a one-lane highway, we begin with the conservation law in differential form

*This work was supported by grants APVV-19-0460, VEGA 1/0709/19 and VEGA 1/0436/20.

†Department of Mathematics, Faculty of Civil Engineering, Slovak University of Technology, Radlinskeho 11, 81368 Bratislava, Slovakia (gergo.ibolya@stuba.sk, karol.mikula@stuba.sk).

$$\rho_t + f_x = 0, \tag{1.2}$$

where ρ is the density and $f = f(\rho)$ is the flux of cars. In our case equation (1.2) represents the conservation of cars. An interesting question is how the flux is related to the density. It is reasonable to expect that a driver in a traffic slows down if the cars are getting closer to each other. In other words, the speed of a car decreases as the density increases. This model was first suggested by Lighthill, Whitham [7] and Richards [8]. One simple example is if we assume that the speed is a linearly decreasing function of the density. This assumption leads to a nonlinear flux function

$$f(\rho) = \rho V_{max}\left(1 - \rho\right), \quad 0 \leq \rho \leq 1$$

where V_{max} is the speed on an empty road. The density is measured in units of cars per car length, for simplicity assuming that every car has the same length. Then $\rho = 1$ and $\rho = 0$ represents bumper to bumper traffic and empty road respectively. A way to improve this model, as stated in [7, 9], is to assume that the flux also depends on the density gradient. If the traffic is getting denser more rapidly the drivers are reducing their speed more. Applying this yields a modified flux function

$$f(\rho, \rho_x) = \rho V_{max}\left(1 - \rho\right) - \sigma\rho_x, \tag{1.3}$$

where σ is a positive constant. Substituting (1.3) to (1.2) and putting the term with a minus sign on the right-hand side we get

$$\rho_t + u(\rho)\rho_x = \sigma\rho_{xx}, \tag{1.4}$$

where we denoted

$$u(\rho) = V_{max}\left(1 - 2\rho\right). \tag{1.5}$$

Multiplying both sides by $u'(\rho)$ we obtain

$$u'(\rho)\rho_t + u'(\rho)u(\rho)\rho_x = u'(\rho)\sigma\rho_{xx},$$

which can be rewritten as

$$u_t + uu_x = \sigma u_{xx} - \sigma u''(\rho)\rho_x^2.$$

Since $u''(\rho) = 0$ we end up with the viscous Burgers' equation (1.1). By solving (1.1) and using the relationship (1.5) we easily obtain a relation for the density

$$\rho(u) = \frac{1}{2}\left(1 - \frac{u}{V_{max}}\right). \tag{1.6}$$

The model discussed above is a simple continuum model of the traffic. Obviously it isn't the most accurate mathematical description of the interactions between cars. However, despite its deficiencies, it gives us valuable insight into how cars are behaving in a traffic. For further discussions of how the Burgers' equation appears in traffic flow models see [9].

2. Numerical scheme. For reader convenience we present here the derivation of the IIOE scheme [3, 4, 5] for the equation

$$u_t + vu_x = 0, \tag{2.1}$$

where $v = v(x)$. We rewrite (2.1) in the equivalent form

$$u_t + (vu)_x - uv_x = 0, \tag{2.2}$$

and integrating over a grid cell p_i with cell center x_i, length h, left border $x_{i-\frac{1}{2}}$, right border $x_{i+\frac{1}{2}}$ yields

$$\int_{p_i} u_t \, dx + \int_{p_i} (vu)_x \, dx - \int_{p_i} uv_x \, dx = 0$$

Let us denote $v_i = v(x_i)$, $v_{i-\frac{1}{2}} = v(x_{i-\frac{1}{2}})$, $v_{i+\frac{1}{2}} = v(x_{i+\frac{1}{2}})$. Let us denote by u_i^n a constant value of the solution inside the i-th finite volume cell at time step n computed by the numerical scheme. We use a constant representation of the solution inside a cell p_i denoted by $\bar{u}_i$ and constant representative values at the cell interfaces denoted by $\bar{u}_{i-\frac{1}{2}}$, $\bar{u}_{i+\frac{1}{2}}$ respectively. Using the Newton-Leibniz formula we obtain

$$\int_{p_i} u_t \, dx + v_{i+\frac{1}{2}} \bar{u}_{i+\frac{1}{2}} - v_{i-\frac{1}{2}} \bar{u}_{i-\frac{1}{2}} - \bar{u}_i (v_{i+\frac{1}{2}} - v_{i-\frac{1}{2}}) = 0.$$

By rearranging terms we get

$$\int_{p_i} u_t \, dx + v_{i-\frac{1}{2}} (\bar{u}_i - \bar{u}_{i-\frac{1}{2}}) + (-v_{i+\frac{1}{2}})(\bar{u}_i - \bar{u}_{i+\frac{1}{2}}) = 0.$$

$v_{i-\frac{1}{2}} > 0$ represents inflow from the left cell interface, while $(-v_{i+\frac{1}{2}}) > 0$ represents inflow from the right cell interface. Otherwise they represent outflows. Thus we define

$$a^{in}_{i-\frac{1}{2}} = \max(v_{i-\frac{1}{2}}, 0), \quad a^{out}_{i-\frac{1}{2}} = \min(v_{i-\frac{1}{2}}, 0),$$
$$a^{in}_{i+\frac{1}{2}} = \max(-v_{i+\frac{1}{2}}, 0), \quad a^{out}_{i+\frac{1}{2}} = \min(-v_{i+\frac{1}{2}}, 0).$$

We use a simple forward finite difference approximation for the time derivative $\frac{u_i^n - u_i^{n-1}}{\tau}$, where τ is a uniform time step, take inflow implicitly, outflow explicitly and use the straightforward reconstructions $\bar{u}_i^n = u_i^n$, $\bar{u}^n_{i-\frac{1}{2}} = \frac{1}{2}(u_i^n + u_{i-1}^n)$, $\bar{u}^n_{i+\frac{1}{2}} = \frac{1}{2}(u_i^n + u_{i+1}^n)$, we obtain the basic one-dimensional IIOE scheme for variable velocity:

$$u_i^n + \frac{\tau}{2h} a^{in}_{i-\frac{1}{2}} \left(u_i^n - u_{i-1}^n\right) + \frac{\tau}{2h} a^{in}_{i+\frac{1}{2}} \left(u_i^n - u_{i+1}^n\right) = \tag{2.3}$$
$$u_i^{n-1} - \frac{\tau}{2h} \left(a^{out}_{i-\frac{1}{2}} \left(u_i^{n-1} - u_{i-1}^{n-1}\right) + a^{out}_{i+\frac{1}{2}} \left(u_i^{n-1} - u_{i+1}^{n-1}\right) \right).$$

For the advective part of (1.1) we use the same derivation as for the 1D variable velocity case but considering the time dependent velocities in the k-th iteration

$$v^{n,k}_{i-\frac{1}{2}} = (u_i^{n,k-1} + u_{i-1}^{n,k-1})/2, \quad v^{n,k}_{i+\frac{1}{2}} = (u_i^{n,k-1} + u_{i+1}^{n,k-1})/2, \quad k = 1, 2, 3, ...$$

and $u_i^{n,0} = u_i^{n-1}$. When solving the traffic flow problem (1.4), instead of u_i^n we calculate ρ_i^n. Using the same reconstructions as for u_i^n, cancelling common factors, the time dependent velocities according to (1.5) in the k-th iteration become

$$v^{n,k}_{i-\frac{1}{2}} = V_{max} \left(1 + (\rho_i^{n,k-1} + \rho_{i-1}^{n,k-1})\right), \quad v^{n,k}_{i+\frac{1}{2}} = V_{max} \left(1 + (\rho_i^{n,k-1} + \rho_{i+1}^{n,k-1})\right).$$

In both cases we consider the time dependent splitting to inflows and outflows

$$a_{i-\frac{1}{2}}^{in,n,k} = \max(v_{i-\frac{1}{2}}^{n,k}, 0), \quad a_{i-\frac{1}{2}}^{out,n} = \min(v_{i-\frac{1}{2}}^{n,1}, 0),$$
$$a_{i+\frac{1}{2}}^{in,n,k} = \max(-v_{i+\frac{1}{2}}^{n,k}, 0), \quad a_{i+\frac{1}{2}}^{out,n} = \min(-v_{i+\frac{1}{2}}^{n,1}, 0).$$

In order to keep second order accuracy of the IIOE scheme, the diffusion part is treated by the Crank-Nicolson approach, and we end up with the following (nonlinear) system

$$u_i^n + \frac{\tau}{2h}\left(a_{i-\frac{1}{2}}^{in,n,k} + \frac{\sigma}{h}\right)\left(u_i^n - u_{i-1}^n\right) + \frac{\tau}{2h}\left(a_{i+\frac{1}{2}}^{in,n,k} + \frac{\sigma}{h}\right)\left(u_i^n - u_{i+1}^n\right) = \tag{2.4}$$
$$u_i^{n-1} - \frac{\tau}{2h}\left(\left(a_{i-\frac{1}{2}}^{out,n-1} + \frac{\sigma}{h}\right)\left(u_i^{n-1} - u_{i-1}^{n-1}\right) + \left(a_{i+\frac{1}{2}}^{out,n-1} + \frac{\sigma}{h}\right)\left(u_i^{n-1} - u_{i+1}^{n-1}\right)\right).$$

This system is solved iteratively updating $a_{i-\frac{1}{2}}^{in,n,k}$ and $a_{i+\frac{1}{2}}^{in,n,k}$ using subsequent values of the iterative solution, starting iterations by u^{n-1}. In every iteration, we calculate the residuum defined as

$$\frac{||A(u^{n,k})u^{n,k} - Bu^{n-1}||}{N},$$

where $A(u^{n,k})$ and B are coefficient matrices obtained by writing the nonlinear system (2.4) using matrix notation and N is the number of unknowns. While solving the Burgers' equation (1.1), the calculation is stopped when the residuum in solving the nonlinear system (2.4) drops below 10^{-6}. To achieve the desired accuracy while solving the traffic flow problem (1.4), we stop the calculation when the residuum drops below 10^{-7}. It means that we have to solve few times (usually from 3 to 6) a tridiagonal system in every time step of the IIOE scheme in case of nonlinear advection problems. The tridiagonal system is solved using the Thomas' algorithm.

3. Numerical experiments. In order to test the numerical scheme (2.4), we chose 4 representative solutions of the Burgers' equation (3.6): the traveling-wave solution, the rarefaction-wave solution, the triangular-wave solution and a trigonometric solution. The traveling-wave solution was first used to test the numerical scheme (2.4) in [3]. Comparisons of the numerical solutions obtained by the IIOE scheme (2.4) with the other three exact solutions are presented here for the first time. These solutions were obtained using the Cole-Hopf transformation, for details see [2]. We present a traveling and rarefaction-wave solution also in the context of traffic flow.

3.1. Traveling wave. First we test the numerical scheme (2.4) on the exact traveling-wave solution

$$u(x,t) = u_r + \frac{1}{2}(u_l - u_r)\left(1 - \tanh\left(\frac{(u_l - u_r)(x - st)}{4\sigma}\right)\right), \tag{3.1}$$

where $u_l > u_r$, $s = (u_l + u_r)/2$. First we solve the problem (1.1) by the scheme (2.4) on space interval (-0.5, 0.5) and in time interval (0, 0.48) with $\sigma = 0.01$. In this test example we chose a time step $\tau = 4h$. It means that for $h = 0.01 (n = 100)$ we use a time step $\tau = 0.04$. Then one can refine the time step and grid size in order to check that the scheme is second order accurate, cf. Table 3.1. The visual comparisons of the numerical and exact solutions for $n = 100$ are presented in Figure 3.1.

If we calculate the inflow coefficients using the values of the solution from the previous time step (number of nonlinear iterations = 1), we get EOC = 1, as it is

documented in Table 3.2. In Figure 3.2 we can observe that the propagation speed of the numerical solution differs from the exact speed. By refining the grid, the speed gets closer to the exact one.

In the second case we decreased the viscosity ten times and use $\sigma = 0.001$. In Table 3.3 we show errors and EOC for refined and coarsened grids and time step. One can again see that EOC=2 also in this example when refining the grid. The lower convergence rate in the beginning is caused by oscillations when the grid size is not sufficiently fine, but as we can see from Figure 3.3 these oscillations are "stable", they do not increase in time and by refining the spatial resolution they are removed completely as documented in Figure 3.4.

As discussed earlier, by making certain assumptions about the flux function, we can transform the solution (3.1) to obtain a solution for the density of the cars in the traffic flow problem (1.4). In the context of traffic flow, a traveling wave is formed as cars are stopping one after the other at the red light. We show this on a simple model example, where the traffic light turns red at position 0.0 and the cars coming from the left are successively stopping behind the car before them. The density of the incoming traffic was chosen to be 0.1, which means that there is one car per 10 times car length. Where the cars are staying, the density is 1, which means bumper to bumper traffic. The exact solution for the density was obtained as follows: we start by choosing $\rho_l = 0.1$ and $\rho_r = 1$, the correspondig values $u_l = 0.8$ and $u_r = -1$ were calculated according to (1.5). Then using the relationship (1.6) we obtain the solution for the density. The traffic flow problem (1.4) was solved numerically using the IIOE scheme (2.4). The errors are documented in Table 3.4. The solution for the red light problem using $\sigma = 0.01$, $V_{max} = 1$ is presented in Figure 3.5.

TABLE 3.1
Report on the L_2 errors of IIOE *method for the traveling-wave solution* (3.1) *of the viscous Burgers' equation* (1.1) *with* $\sigma = 0.01$.

n	h	τ	NTS	$L_2(I, L_2)$	EOC
100	0.01	0.04	12	$5.0\ 10^{-3}$	
200	0.005	0.02	24	$1.22\ 10^{-3}$	2.03
400	0.0025	0.01	48	$3.03\ 10^{-4}$	2.01
800	0.00125	0.005	96	$7.74\ 10^{-5}$	1.97
1600	0.000625	0.025	192	$1.90\ 10^{-5}$	2.02

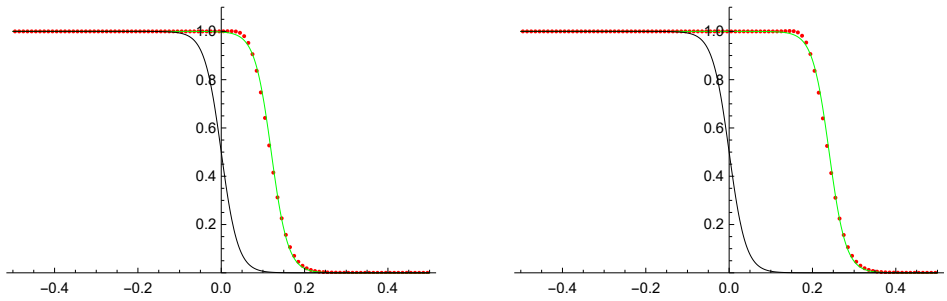

FIG. 3.1. *Comparing the* IIOE *scheme with the exact traveling-wave solution* (3.1) *in time* $t = 0.24$ *(left) and* $t = 0.48$ *(right), with* $\sigma = 0.01$, $n = 100$, $\tau = 4h$

TABLE 3.2

Report on the L_2 errors of IIOE *method for the traveling-wave solution* (3.1) *of the viscous Burgers' equation* (1.1) *with $\sigma = 0.01$, number of nonlinear iterations = 1.*

n	h	τ	NTS	$L_2(I, L_2)$	EOC
100	0.01	0.04	12	$4.41\ 10^{-2}$	
200	0.005	0.02	24	$2.32\ 10^{-2}$	0.93
400	0.0025	0.01	48	$1.18\ 10^{-2}$	0.97
800	0.00125	0.005	96	$5.96\ 10^{-3}$	0.99

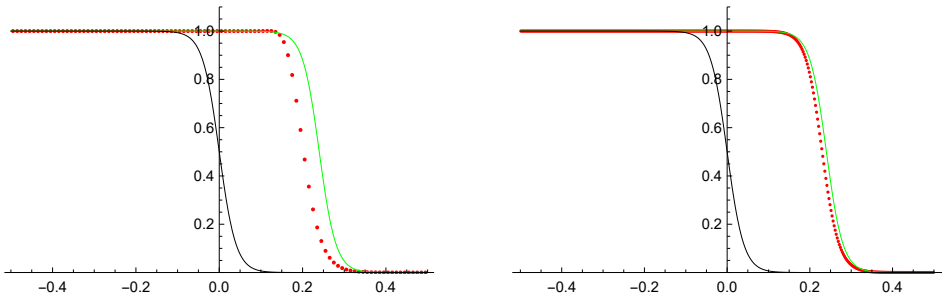

FIG. 3.2. *Comparing the* IIOE *scheme with the exact traveling-wave solution* (3.1) *in time $t = 0.48$, with $\sigma = 0.01$, $n = 100$(left), $n = 400$(right), $\tau = 4h$, number of nonlinear iterations = 1. We can see that after refining the grid, the propagation speed of the numerical solution is getting closer to the exact speed.*

TABLE 3.3

Report on the L_2 errors of IIOE *method for the traveling-wave solution* (3.1) *of the viscous Burgers' equation* (1.1) *with $\sigma = 0.001$.*

n	h	τ	NTS	$L_2(I, L_2)$	EOC
250	0.004	0.016	30	$2.01\ 10^{-2}$	
500	0.002	0.08	60	$6.84\ 10^{-3}$	1.55
1000	0.001	0.04	120	$1.79\ 10^{-3}$	1.94
2000	0.0005	0.02	240	$4.55\ 10^{-4}$	1.97

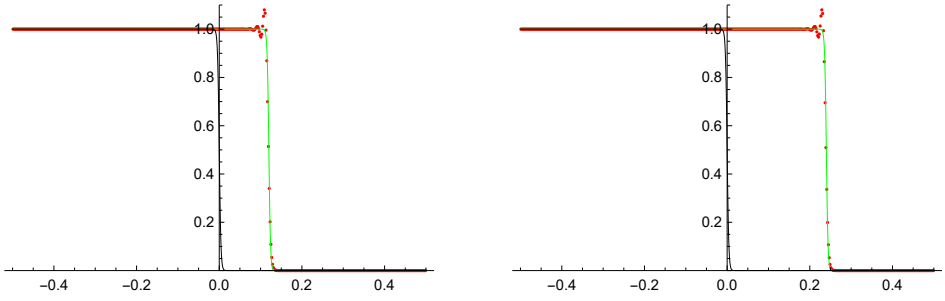

FIG. 3.3. *Comparing the* IIOE *scheme with the exact traveling-wave solution* (3.1) *in time $t = 0.24$ (left) and $t = 0.48$ (right), with $\sigma = 0.001$, $n = 500$, $\tau = 4h$. We can observe small nonincreasingly propagating oscillations.*

3.2. Rarefaction wave. Our next example is the exact rarefaction wave solution

$$u(x,t) = u_l + \frac{u_r - u_l}{1 + e^{(u_r - r_l)(x-st)/2\sigma} \operatorname{erfc}\left(\frac{x-u_l t}{2\sqrt{\sigma t}}\right) \Big/ \operatorname{erfc}\left(\frac{u_r t - x}{2\sqrt{\sigma t}}\right)}, \tag{3.2}$$

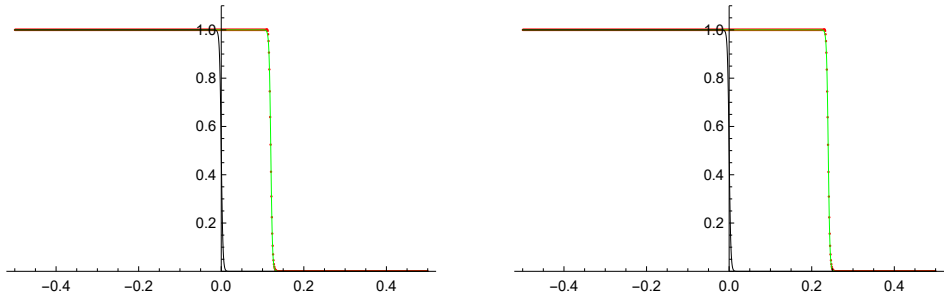

FIG. 3.4. *Comparing the* IIOE *scheme with the exact traveling-wave solution* (3.1) *in time* $t = 0.24$ *(left) and* $t = 0.48$ *(right), with* $\sigma = 0.001$, $n = 1000$, $\tau = 4h$. *On the refined grid the oscillations are gone.*

TABLE 3.4
Report on the L_2 *errors of* IIOE *method for the traffic flow problem* (1.4) *with* $\sigma = 0.01$.

n	h	τ	NTS	$L_2(I, L_2)$	EOC
100	0.01	0.04	12	$9.82\ 10^{-4}$	
200	0.005	0.02	24	$2.36\ 10^{-4}$	2.05
400	0.0025	0.01	48	$5.94\ 10^{-5}$	1.99
800	0.00125	0.005	96	$1.53\ 10^{-5}$	1.96

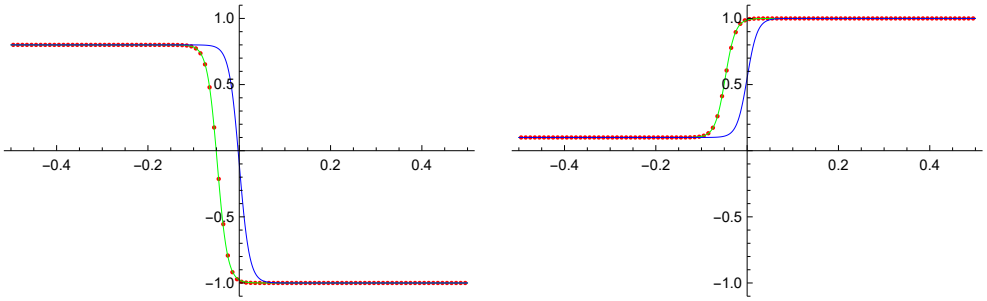

FIG. 3.5. *Solution for the red light problem. At* $t = 0$ *the light turns red at position* 0.0 *and the incoming cars from left are stopping one after the other. At time* $t = 0$ *the exact solution of the traffic flow problem* (1.4) *for the density(right) with* $\sigma = 0.01$ *is plotted. It was obtained by transforming the traveling-wave solution* (3.1) *of the Burgers' equation* (1.1)*(left) using* (1.6). *In our case,* $\rho_l = 0.1$, $\rho_r = 1$. *The corresponding values for the traveling-wave solution* (3.1) *calculated using* (1.5) *are* $u_l = 0.8$, $u_r = -1$. *The results of the numerical solution (red) for the Burgers' equation (1.1) (left) and the density(right) by the* IIOE *scheme are shown at time* $t = 0.48$.

where $u_l < u_r$, $s = (u_l + u_r)/2$. First, equation (1.1) is solved by the scheme (2.4) on space interval (-0.5, 0.5) and time interval (0.01, 0.41) with $\sigma = 0.01$. Since the exact solution (3.2) is defined for $t > 0$, we decided to initialize the calculation at time 0.01. The time step τ was chosen to be equal to $4h$ again. The numerical solution is visually compared to the exact solution in Figure 3.6. The errors are presented in Table 3.5.

This solution also has an interesting interpretation in a context of traffic flow. Imagine that the road is divided into two parts by the traffic light positioned at 0.0. At the beginning the density on the left part equals to 1 and there is an empty

road on the right. At time $t = 0$ the light turns green at position 0.0 and cars are accelerating smoothly, the traffic rarifies. The exact solution for the density in (1.4) was obtained the same way as in our previous example. First, considering the values $\rho_l = 1$, $\rho_r = 0$ we calculate the corresponding values $u_l = -1$, $u_r = 1$ according to (1.5). Then substituting the exact solution (3.2) to (1.6) we get the density function. The numerical solution for the density by the IIOE scheme (2.4) is presented for $\sigma = 0.001$, $V_{max} = 1$ in Figure 3.7.

TABLE 3.5

Report on the L_2 errors of IIOE *method for the rarefaction-wave solution* (3.2) *of the viscous Burgers' equation* (1.1) *with* $\sigma = 0.01$.

n	h	τ	NTS	$L_2(I, L_2)$	EOC
100	0.01	0.04	10	$5.48\ 10^{-3}$	
200	0.005	0.02	20	$1.56\ 10^{-3}$	1.82
400	0.0025	0.01	40	$4.01\ 10^{-4}$	1.96
800	0.00125	0.005	80	$1.00\ 10^{-4}$	2.00

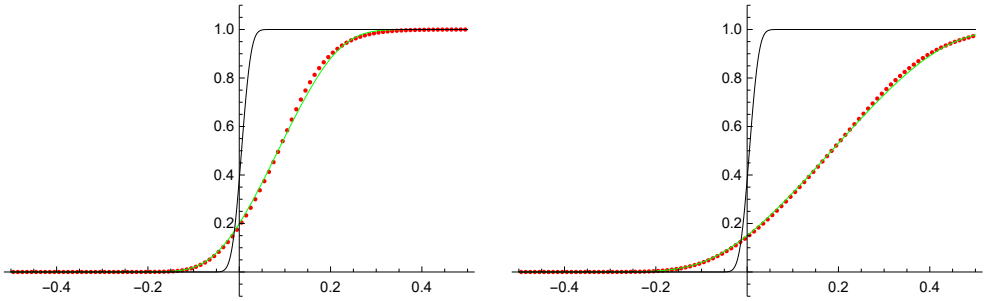

FIG. 3.6. *Comparing the* IIOE *scheme with the exact rarefaction-wave solution* (3.2) *in time* $t = 0.17$ *(left) and* $t = 0.41$ *(right), with* $\sigma = 0.01$, $n = 100$, $\tau = 4h$

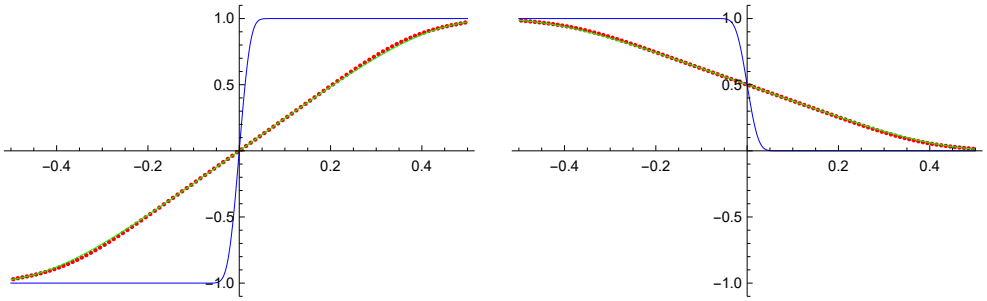

FIG. 3.7. *Solution for the green light problem. At* $t = 0$ *the light turns green at position* 0.0 *and cars are accelerating smoothly from left to right. At time* $t = 0.01$*(when the calculation was initialized) the exact solution of the traffic flow problem* (1.4) *for the density(right) with* $\sigma = 0.01$ *is plotted. It was obtained by transforming the rarefaction-wave solution* (3.2) *(left) of the Burgers' equation* (1.1) *using* (1.6). *In this problem,* $\rho_l = 1$, $\rho_r = 0$. *The corresponding values for the rarefaction-wave solution* (3.2) *calculated using* (1.5) *are* $u_l = -1$, $u_r = 1$. *The results of the numerical solution for the Burgers' equation* (1.1) *(left) the density (right) by the* IIOE *scheme(red) is shown at time* $t = 0.37$.

3.3. Triangular wave. Another interesting example is the triangular-wave solution

$$u(x,t) = 2\sqrt{\frac{\sigma}{\pi t}}\,\frac{e^{-x^2/4\sigma t}}{\coth\left(\frac{1}{4\sigma}\right) - \operatorname{erf}\left(\frac{x}{2\sqrt{\sigma t}}\right)}. \tag{3.3}$$

In this case the problem (1.1) is solved by the scheme (2.4) on space interval (-0.5, 1.5) and time interval (0.01, 0.51) with $\sigma = 0.01$. Again, as in the previous case of the rarefaction wave solution (3.2), the exact solution (3.3) is defined for $t > 0$ so the numerical calculation was initialized at time 0.01. In Table 3.6 we show the errors for refined grids and time step. When the grid size is not sufficiently fine, we can observe oscillations at the peak of the wave. These oscillations do not grow unboundedly and can be removed by refining the grid as it is shown in Figure 3.8.

TABLE 3.6
Report on the L_2 errors of IIOE *method for the triangular-wave solution* (3.3) *of the viscous Burgers' equation* (1.1) *with* $\sigma = 0.02$.

n	h	τ	NTS	$L_2(I, L_2)$	EOC
100	0.02	0.08	5	$3.07\ 10^{-1}$	
200	0.01	0.04	10	$1.30\ 10^{-1}$	1.24
400	0.005	0.02	20	$3.72\ 10^{-2}$	1.81
800	0.0025	0.01	40	$9.02\ 10^{-3}$	2.04

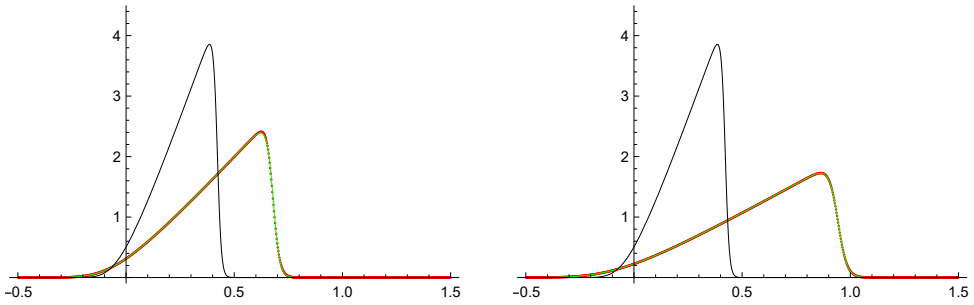

FIG. 3.8. *Comparing the* IIOE *scheme with the exact triangular wave solution* (3.3) *in time* $t = 0.26$ *(left),* $t = 0.50$ *(right) for* $n = 800$ *whith* $\sigma = 0.02$, $\tau = 4h$.

3.4. Trigonometric solution. Our last example is the trigonometric solution

$$u(x,t) = \frac{2\sigma b\pi \sin \pi x}{ae^{\sigma\pi^2 t} + b\cos \pi x}, \tag{3.4}$$

where a and b are constants, $a > b$. The errors are reported in Table 3.7. A visual comparison of the numerical results with the exact solution is presented in Figure 3.9.

4. Conclusions. In this article, the numerical solution of the viscous Burgers' equation (1.1) and the traffic flow problem (1.4) by the IIOE scheme (2.4) was presented. Numerical experiments were performed on uniform grids and have shown the second order convergence of the presented IIOE method.

TABLE 3.7

Report on the L_2 errors of IIOE *method for the trigonometric solution* (3.4) *of the viscous Burgers' equation* (1.1) *with* $\sigma = 0.01$.

n	h	τ	NTS	$L_2(I, L_2)$	EOC
100	0.02	0.08	15	$1.66\ 10^{-2}$	
200	0.01	0.04	30	$3.18\ 10^{-3}$	2.38
400	0.005	0.02	60	$5.30\ 10^{-4}$	2.58
800	0.0025	0.01	120	$1.00\ 10^{-4}$	2.41

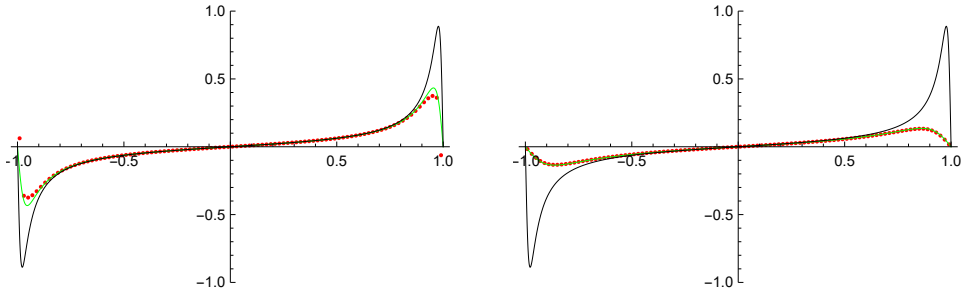

FIG. 3.9. *Comparing the* IIOE *scheme with the exact trigonometric solution* (3.4) *in time* $t = 0.08$ *(left) and* $t = 0.96$ *(right) for* $n = 100$, *with* $\sigma = 0.01$, $b = 1$, $a = 1.0025$, $\tau = 4h$.

Acknowledgments. We thank to Mario Ohlberger who co-authored preprint [3] in which the IIOE method for nonlinear advection problem was presented for the first time but never published before this article.

REFERENCES

[1] R.J. LEVEQUE, *Finite Volume Methods for Hyperbolic Problems*, Cambridge Texts in Applied Mathematics. Cambridge University Press, 2002.
[2] P. J. OLVER, *Introduction to Partial Differential Equations*, Undergraduate Texts in Mathematics. Springer, New York, 2014.
[3] K. MIKULA, M. OHLBERGER, *A new Inflow-Implicit/Outflow-Explicit Finite Volume Method for Solving Variable Velocity Advection Equations*, Preprint 01/10 - N, Angewandte Mathematik und Informatik, Universitaet Münster, June 2010
[4] K. MIKULA, M. OHLBERGER, *Inflow-Implicit/Outflow-Explicit Scheme for Solving Advection Equations*, in Finite Volumes in Complex Applications VI, Problems & Perspectives, Eds.J.Fořt et al. (Proceedings of the Sixth International Conference on Finite Volumes in Complex Applications, Prague, June 6-10, 2011), Springer Verlag, 2011, pp. 683-692.
[5] K. MIKULA, M. OHLBERGER, J.URBAN, *Inflow-Implicit/Outflow-Explicit finite volume methods for solving advection equations*, Applied Numerical Mathematics, Vol. 85 (2014) pp. 16-37
[6] B. N. GREENSHIELDS, *A study of traffic capacity*, In Proceedings of the 14th Annual Meeting of the Highway Research Board, 1934, pp. 448-474.
[7] M. J. LIGHTHILL AND G. B. WHITHAM, *On kinematic waves II: A theory of traffic flow on long crowded roads*, Proc. Roy. Soc. London Ser. A, (1955), pp. 317-345.
[8] P. I. RICHARDS, *Shock waves on highways*, Oper. Res., 4 (1956), pp. 42-51.
[9] G. B. WHITHAM, *Linear and Nonlinear Waves*, Wiley-Interscience, 1974.